

Perpendicular giant magnetoresistance of multilayered Co/Cu nanowires

K. Liu

Department of Physics and Astronomy, The Johns Hopkins University, Baltimore, Maryland 21218

K. Nagodawithana and P. C. Searson

Department of Materials Science and Engineering, The Johns Hopkins University, Baltimore, Maryland 21218

C. L. Chien

Department of Physics and Astronomy, The Johns Hopkins University, Baltimore, Maryland 21218

(Received 16 November 1994)

We have successfully fabricated multilayered Co/Cu nanowires with different diameters and various layer thicknesses by electrodeposition. They display a large perpendicular giant magnetoresistance up to 11% at room temperature and 22% at 5 K. The spin-flip diffusion length has been directly measured to be about 210 Å for this system.

Recently, the phenomenon of giant magnetoresistance (GMR) has attracted a great deal of attention for fundamental interest and technological applications. GMR was discovered in certain Fe/Cr structures,¹ and subsequently in other multilayers in which the interlayer exchange coupling results in an antiferromagnetic alignment of the adjacent magnetic layers.^{2,3} The later observation of GMR in granular systems offers another medium with which GMR can be realized.^{4,5} To date, materials that exhibit GMR have been made mostly by sputtering and molecular-beam epitaxy (MBE), which require high or ultrahigh vacuum. Recent advances in electrochemical techniques⁶ have shown that multilayers^{7,8} and arrays of nanowires⁹ can be deposited from solutions at ambient temperature and pressure. In this work, we report the fabrication of nanowires of multilayers, and the observation of GMR in such materials.

In multilayers, GMR can be observed more commonly in the current-in-plane (CIP) geometry, whereas that of current-perpendicular-plane (CPP) geometry is much more difficult because of the extremely small resistance involved. The only successful experiments on CPP GMR utilize either a sensitive superconducting-quantum-interference-device-based system on multilayers with approximately 1 mm² in cross section,³ or microlithographically structured pillars with 6–130 μm² in cross section.¹⁰ Arrays of nanowires with multilayers are another medium that provides a CPP geometry, with cross sections as small as 700 nm², which is more than four orders of magnitude smaller.

Sample fabrication begins with Nuclepore polycarbonate membranes of two kinds: membrane thickness = 6 μm, pore size = 30 nm, with a pore density = 6 × 10⁶ pores/mm²; membrane thickness = 10 μm, pore size = 400 nm, with a pore density = 10⁶ pores/mm². A thin Cu layer (~0.3 μm thick) is sputter-deposited onto one side of the membrane and used as the working electrode in a standard three-electrode electrochemical cell.⁹ The electrolyte, confined to the other side of the membrane, contains 50 g/liter Co in the form of cobalt (II) sulfate heptahydrate, 0.5 g/liter Cu in the form of copper (II) sulfate pentahydrate, and 40 g/liter boric acid. Cu and Co were deposited at -0.16 and -1.00 V,

respectively, relative to the Ag⁺/AgCl reference electrode. At -0.16 V, only Cu is deposited, whereas at -1.00 V, both metals are codeposited. However, because the Cu concentration in the solution is so low, the deposition of Cu is diffusion limited. Therefore, with a fast Co deposition (e.g., in 400-nm pores, the deposition rate of Co is about 60 Å/s, fifteen times higher than that of Cu), only a small amount of Cu is codeposited in the Co layer. Depositions at -1.00 V onto Si wafers sputter-coated with Ag show about 7 at. % Cu impurities in Co as determined by energy dispersive x-ray microanalysis (EDX). The compromise between a reasonably fast deposition rate and a tolerable impurity level has led us to the growth conditions.

During deposition, the applied potential is set by a potentiostat controlled by a coulometer, which integrates the amount of charge passing between the working electrode and the counter electrode. The potential is switched when the amount of charge corresponding to a designed layer thickness is reached. Calibrations of the Co and Cu deposition efficiencies have been carried out separately, on Ag-coated Si, by comparing the actual weight of the material deposited with that calculated from the recorded charge. This procedure takes into account that hydrogen evolution occurred during the deposition process, primarily in Co plating, which also contributes to the charge accumulation monitored by the coulometer. Another precaution taken is a few seconds open-circuit interruption during the transition from Co to Cu deposition⁸ to avoid severe Co dissolution during the copper deposition cycle which could damage the interface and leave the Co layer thickness inaccurate.

Our initial test run has been carried out by growing Co/Cu multilayers on Ag-coated Si. Figure 1 shows the small-angle x-ray diffraction pattern of a [Co(48 Å)/Cu(30 Å)]₂₀₀ sample. Diffraction peaks up to seventh order have been observed, indicating good multilayer quality. The bilayer thickness determined from the peak positions is $L = 80$ Å, matching the designed value. Magnetic measurements performed on a vibrating sample magnetometer reveal the expected shape anisotropy with an in-plane easy axis. For the fabrication of the arrays of nanowires, deposition is initiated from within the pores onto the sputtered Cu film and continues until the

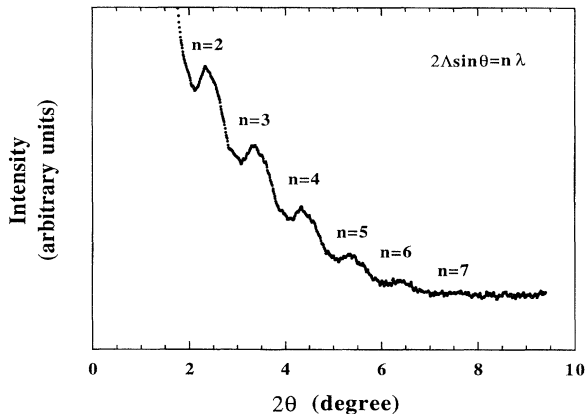


FIG. 1. Small-angle x-ray diffraction pattern of a $[\text{Co}(48 \text{ \AA})/\text{Cu}(30 \text{ \AA})]_{200}$ sample grown on Ag-coated Si.

pores are completely filled. For all samples, the Co layer thickness has been kept at 50 \AA , while the Cu layer thickness has been varied from a few to several hundred angstroms. With the 6- or $10\text{-}\mu\text{m}$ -thick membranes, the nanowires thus made contain several hundred to a few thousand bilayers.

A scanning electron microscope (SEM) micrograph of the top view of a membrane with 400-nm pores is shown in Fig. 2(a). An SEM micrograph of the 400-nm nanowire arrays, after the polycarbonate membrane has been etched away, is shown in Fig. 2(b). The poorly aligned nanowires shown in Fig. 2(b) are due to the loss of support from the membrane. Transmission electron microscopy (TEM) is used to study the structure and morphology of the layered nanowires removed from the membrane. Figure 2(c) shows a TEM picture of a free-standing 30-nm -diameter nanowire of $[\text{Co}(50 \text{ \AA})/\text{Cu}(20 \text{ \AA})]_{850}$. Because of the intrinsically poor contrast between Co and Cu, the multilayer nature of the nanowire is only partially illustrated. Electron diffraction patterns obtained from the individual grains show that they are polycrystalline. X-ray diffraction has also been used to study the structure of the nanowires with the sputtered Cu electrodes etched away. The spectrum shows only an fcc structure, indicating that the multilayers are fcc Co/fcc Cu, the same as that in bulk Co/Cu multilayers fabricated by vacuum deposition.

Caution has been exercised with regard to resistance and magnetoresistance measurements. After the completion of the deposition of the Co/Cu multilayers in the nanowires, the potential is fixed at -0.16 V in order to cap each nanowire with Cu. After suitable cleaning of the top membrane surface, another Cu layer is then sputtered onto the Cu caps to electrically connect all of them. Using a simple photoresist technique, the Cu layers are etched away except a thin strip ($\sim 100 \mu\text{m}$) remains, and that the two Cu strips on the top and the bottom surface of the membrane are perpendicular to each other. Because many Cu caps tend to fall off in these additional processes, we have used SEM to determine the number of nanowires (~ 200) within the overlapping region ($\sim 100 \times 100 \mu\text{m}^2$) between the two perpendicular Cu strips that are connected to both Cu strips. Current leads and voltage leads are attached to the Cu strips using Ag epoxy. The typical resistance of the 30- and 400-nm -diameter nanowires thus measured is on the 10- and $10^{-2}\text{-}\Omega$ scale, respectively.

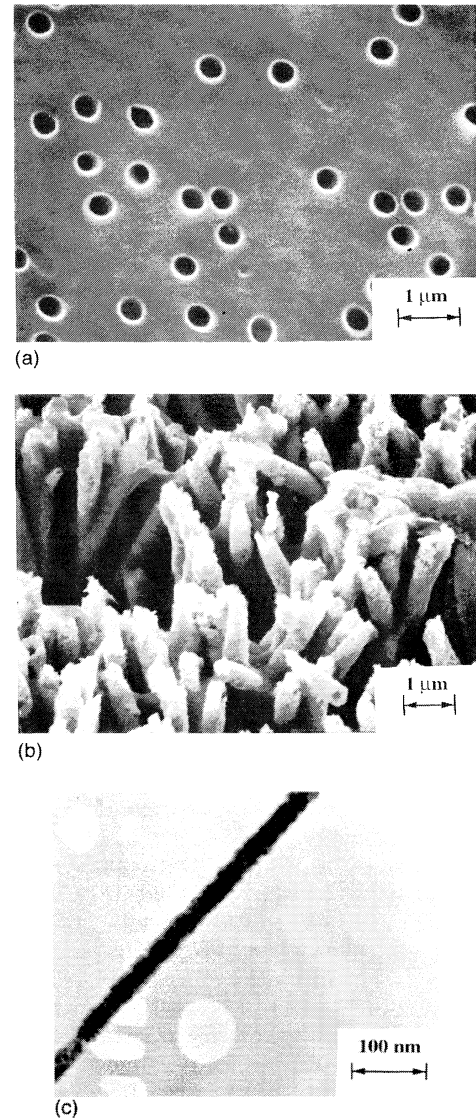


FIG. 2. (a) Top-view SEM image of a membrane with 400-nm pores, (b) SEM image of 400-nm multilayered nanowires with the membrane removed, (c) TEM picture of a free-standing 30-nm -diameter nanowire with layered structure $[\text{Co}(50 \text{ \AA})/\text{Cu}(20 \text{ \AA})]_{850}$.

Figure 3 shows the GMR results of $[\text{Co}(50 \text{ \AA})/\text{Cu}(8 \text{ \AA})]_{1000}$, typical of the 30-nm nanowires, at room temperature and 5 K with field perpendicular to wires. At room temperature, 11% GMR (with respect to the saturation resistance R_s at 50 kOe) is observed with a zero-field resistance of 38Ω , with no discernible hysteretic characteristics. At 5 K , GMR of 22% with hysteretic behavior is observed. The initial resistance at $H=0$ is noticeably larger than the field-cycle MR, a feature commonly observed in GMR materials particularly in the CPP geometry.³ It is also noticed that the coercive field (H_c) of the magnetic hysteresis loop is smaller than H_M , at which MR reaches the maximum. The saturation field (H_s) increases from 1.8 kOe at room temperature to 3.7 kOe at 5 K .

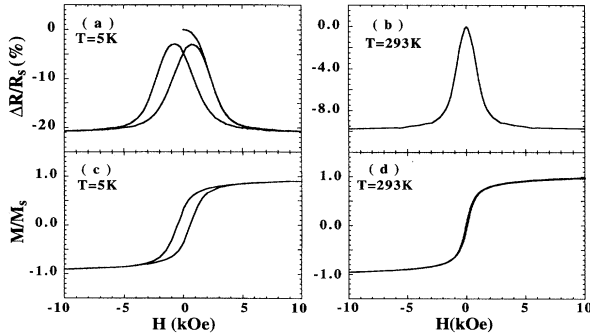


FIG. 3. Magnetoresistance measurements at (a) 5 K and (b) 293 K of 30-nm nanowires with layered structure $[\text{Co}(50 \text{ \AA})/\text{Cu}(8 \text{ \AA})]_{1000}$. The applied magnetic field is perpendicular to the wire. The corresponding magnetic hysteresis loops at (c) 5 K and (d) 293 K are also shown.

The temperature dependence of the resistance and GMR has been studied by measuring the sample resistance in zero field where the resistance is maximum and at 50 kOe where the resistance is saturated. In the CIP Co/Cu GMR measurements, the decrease of GMR ($\Delta R/R$) with increasing temperature is mainly due to the temperature dependence of the resistance (R), whereas the resistance change (ΔR) is essentially temperature independent.² In the present case, as shown in Fig. 4, both R and ΔR have fairly strong temperature dependence. In particular, R increases and ΔR decreases linearly with T .

The critical length scale of the GMR effect in CPP geometry is the spin-flip diffusion length (l_{sf}),^{11,12} over which the conduction electron spin is relaxed. When the Cu layer thick-

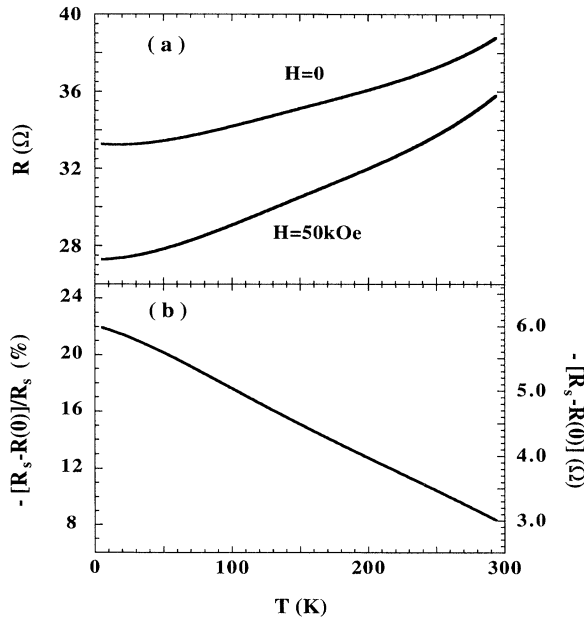


FIG. 4. Temperature dependence of (a) the resistance (R), (b) the change of resistance ($-[R_s - R(0)]$), and percentage change of resistance ($-[R_s - R(0)]/R_s$) of 30-nm $[\text{Co}(50 \text{ \AA})/\text{Cu}(20 \text{ \AA})]_{850}$, where $R(0)$ and R_s are the resistance at 0- and 50-kOe field.

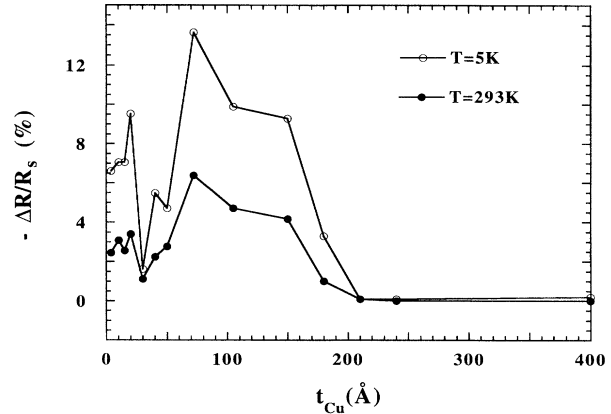


FIG. 5. The GMR effect of 400-nm $[\text{Co}(50 \text{ \AA})/\text{Cu}(t_{\text{Cu}})]_n$ multilayered nanowires at 5 and 293 K as a function of the Cu layer thickness (t_{Cu}).

ness exceeds the spin-flip diffusion length, the conduction electrons would not remember the spin disorder as they pass through adjacent Co layers. The Cu layer thickness (t_{Cu}) at which GMR diminishes to zero should be regarded as a reasonable measure for the spin-flip diffusion length. We have studied a series of 400-nm nanowires with a fixed Co layer thickness of 50 Å and various Cu layer thicknesses. Figure 5 shows the GMR at 5 and 293 K of these samples as a function of Cu thickness. Figure 5 clearly shows, for large Cu thicknesses ($t_{\text{Cu}} > 100 \text{ \AA}$), the GMR effect decreases with increasing t_{Cu} , and approaches zero when $t_{\text{Cu}} \approx 210 \text{ \AA}$, and remains so for larger t_{Cu} . This value of 210 Å directly measures the crucial spin-flip diffusion length. From the data at 5 and 293 K, shown in Fig. 5, the value of l_{sf} is essentially temperature independent.

Also shown in Fig. 5, for smaller Cu thicknesses ($t_{\text{Cu}} < 100 \text{ \AA}$), there appears to be clear oscillations of the GMR effect, a phenomenon well established in sputtered² and MBE-grown¹³ Co/Cu multilayers. However, in the present case, the layered structure, the purity of the layers, and the sharpness of the interfaces have been partly tainted by the electrodeposition process. Before the electrodeposition process is further perfected, although such oscillations are clearly noted, its significance remains to be further explored.

Because of the known contamination of the Co layers with several percent of Cu, it is essential to establish that the GMR effect is due to the multilayer structure in the nanowires. A series of *alloyed* Co-Cu samples have been fabricated using the same process except with a *single* deposition potential, intermediate between -0.16 and -1.00 V , which leads to the codeposition of Co and Cu. Different compositions of Co-Cu alloys with 0, 20, 35, 40, and 92 at. % Co have been made. *None* of the Co-Cu alloy samples shows any GMR effect, except the expected and very small anisotropic MR effect ($< 1\%$). These measurements conclusively demonstrate that the observed GMR in nanowires is intimately related to the layered structure.

As to the mechanism of GMR, it is well established that spin disorder within some characteristic length scale (spin-flip diffusion length for the CPP geometry) is essential to GMR. There are generally two ways to realize the spin dis-

order, using either antiferromagnetic interlayer exchange coupling or uncorrelated magnetic moments. For our multilayered nanowires, in the thin Cu layer thickness regime ($t_{\text{Cu}} < 30 \text{ \AA}$), the antiferromagnetic interlayer exchange coupling is expected to be responsible for GMR. For samples with t_{Cu} in this regime, the saturation fields (H_s) all have substantial increases from room temperature to 5 K. As the saturation field is intimately related to the antiferromagnetic interlayer exchange coupling strength (J) via $H_s = -4J/M_s t_F$, where M_s is the saturation magnetization and t_F is the magnetic layer thickness, the change in H_s indicates a temperature sensitive interlayer exchange coupling. As Cu layer thickness becomes larger ($t_{\text{Cu}} > 30 \text{ \AA}$), the interlayer exchange coupling is expected to become very weak and GMR diminishes according to this mechanism. Therefore, the large GMR effect for $t_{\text{Cu}} > 30 \text{ \AA}$ should be credited to the other mechanism of uncorrelated magnetic moments. The probable scenario is that when $t_{\text{Cu}} > 30 \text{ \AA}$, as the interlayer coupling becomes too weak, the magnetic moments in the adjacent Co layers become uncorrelated. The contribution to GMR from uncoupled moments persists to even $t_{\text{Cu}} \geq 150 \text{ \AA}$, where any antiferromagnetic interlayer exchange coupling has surely died out. At even larger Cu layer thicknesses, a terminating factor for GMR, the spin-flip diffusion length l_{sf} , sets in. The eventual disappearance of GMR at $t_{\text{Cu}} \approx 210 \text{ \AA}$ therefore directly measures the spin-flip diffusion length.

We have also looked into the nanowire resistance. For example, in the case of the 30-nm-diameter multilayered $[\text{Co}(50 \text{ \AA})/\text{Cu}(20 \text{ \AA})]_{850}$ nanowire, we have found a resistance per nanowire of about 10^4 \Omega . If one uses the resistivity values of 5.8×10^{-8} and $1.7 \times 10^{-8} \text{ \Omega m}$ for bulk Co and Cu, respectively, each nanowire would have a resistance of 400 Ω . The main contribution to the extra resistance then should be due to interface resistance. Lee *et al.*,¹² using CPP geometry, found AR_T to be about $5 \times 10^{-16} \text{ \Omega m}^2$ for sputtered

Co/Cu, where R_T is the resistance per interface and A is the cross section. In the present case, if we attribute all the extra resistance to interface resistance, we obtain $40 \times 10^{-16} \text{ \Omega m}^2$ per interface, roughly eight times larger. While in the case of 400-nm-diameter multilayered $[\text{Co}(50 \text{ \AA})/\text{Cu}(105 \text{ \AA})]_{650}$ nanowire, we have found a single-wire resistance of about 26 Ω . When the same treatment is applied, we find AR_T to be about $23 \times 10^{-16} \text{ \Omega m}^2$, again more than four times larger than the value of Lee *et al.*, but smaller than that found in the 30-nm case. We believe boundary scattering effects arising from the extremely small wire diameters have played an important role, as indicated clearly by the further resistance enhancement observed in 30-nm nanowire samples. The values of AR_T most likely have been overestimated because the contributions due to boundary scattering effects as well as impurity scattering have not been taken into exact account. Nevertheless, these results show that the overall resistivity of the multilayered nanowires is considerably higher than those of vacuum-deposited multilayers. This fact is reflected in the smaller spin-flip diffusion length observed, as well as its lack of appreciable temperature dependence.

In conclusion, we have successfully fabricated multilayered Co/Cu nanowires by electrodeposition and have studied their structural characteristics. We have observed a large perpendicular GMR effect, and directly determined the crucial spin-flip diffusion length of about 210 \AA . We have demonstrated a medium, different from multilayers and granular solids, where GMR can be explored using electrodeposition process. This process also provides a simple and effective way to achieve large perpendicular GMR effect, which is of importance in both practical applications and fundamental interest.

Note added. Recently, two studies on the GMR effect of multilayered Co/Cu nanowires^{14,15} have appeared.

The authors acknowledge support from NSF (Grant No. ECS 92-02222) and AESF (Grant No. 86).

¹M. N. Baibich *et al.*, Phys. Rev. Lett. **61**, 2472 (1988).

²S. S. P. Parkin, R. Bhadra, and K. P. Roche, Phys. Rev. Lett. **66**, 2152 (1991).

³W. P. Pratt, Jr. *et al.*, Phys. Rev. Lett. **66**, 3060 (1991); S.-F. Lee *et al.*, Phys. Rev. B **46**, 548 (1992).

⁴A. E. Berkowitz *et al.*, Phys. Rev. Lett. **68**, 3745 (1992).

⁵J. Q. Xiao, J. S. Jiang, and C. L. Chien, Phys. Rev. Lett. **68**, 3749 (1992).

⁶P. C. Searson and T. P. Moffat, Crit. Rev. Surf. Chem. **3**, 171 (1994).

⁷L. H. Bennett *et al.*, Phys. Rev. B **40**, 4633 (1989).

⁸R. D. McMichael *et al.*, J. Magn. Magn. Mater. **113**, 149 (1992).

⁹T. M. Whitney *et al.*, Science **261**, 1316 (1993).

¹⁰M. A. M. Gijs, S. K. J. Lenczowski, and J. B. Giesbers, Phys. Rev. Lett. **70**, 3343 (1993).

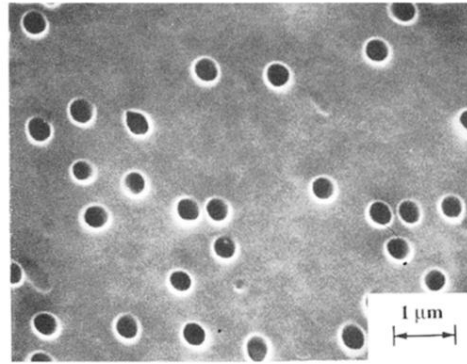
¹¹See, e.g., S. Zhang and P. M. Levy, J. Appl. Phys. **69**, 4786 (1991).

¹²S.-F. Lee *et al.*, J. Magn. Magn. Mater. **118**, 1 (1993).

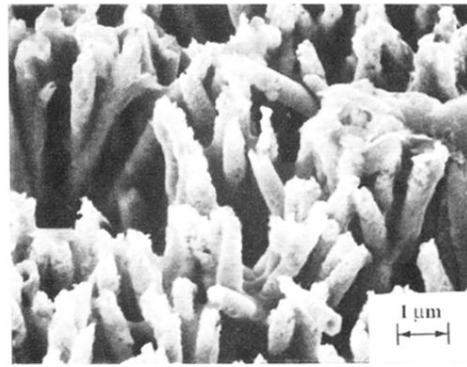
¹³M. Johnson *et al.*, Phys. Rev. Lett. **68**, 2688 (1992).

¹⁴L. Piraux *et al.*, Appl. Phys. Lett. **65**, 2484 (1994).

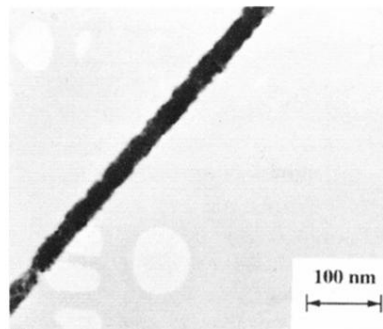
¹⁵A. Blondel *et al.*, Appl. Phys. Lett. **65**, 3019 (1994).



(a)



(b)



(c)

FIG. 2. (a) Top-view SEM image of a membrane with 400-nm pores, (b) SEM image of 400-nm multilayered nanowires with the membrane removed, (c) TEM picture of a free-standing 30-nm-diameter nanowire with layered structure $[\text{Co}(50 \text{ \AA})/\text{Cu}(20 \text{ \AA})]_{850}$.